

An Example of Supercooled Drizzle Drops Formed through a Collision-Coalescence Process

STEWART G. COBER, J. WALTER STRAPP, AND GEORGE A. ISAAC

Cloud Physics Research Division, Atmospheric Environment Service, Downsview, Ontario, Canada

(Manuscript received 26 October 1995, in final form 21 May 1996)

ABSTRACT

The microphysics associated with observations of supercooled drizzle drops, which formed through a condensation and collision-coalescence process, are reported and discussed. The growth environment was an 1100-m-thick stratiform cloud with cloud-base and cloud-top temperatures of -7.5° and -12°C , respectively. The cloud was characterized by a low droplet concentration of 21 cm^{-3} and a large droplet median volume diameter of $29\text{ }\mu\text{m}$, with a concentration of interstitial aerosol particles of less than 15 cm^{-3} (larger than $0.13\text{ }\mu\text{m}$ in diameter). The evolution of drizzle drops was traced downward from cloud top, with a maximum diameter of $500\text{ }\mu\text{m}$ observed at cloud base. The air mass was sufficiently clean to ensure only a small number of active cloud condensation nuclei. Consequently, small concentrations of cloud droplets led to concentrations of over 300 L^{-1} for droplets larger than $40\text{ }\mu\text{m}$, which set up strong conditions for continued growth by collision-coalescence. Ice crystals in concentrations of 0.08 L^{-1} were measured simultaneously with the drizzle drops and were not effective in glaciating the cloud, even though the drizzle drops were estimated to have taken at least 1–2 h to form.

While the growth of precipitation-sized drops through collision-coalescence has been well documented, there are few measurements of this phenomena at temperatures less than 0°C . This study provides a well-documented example of such an event at subfreezing temperatures. The applicability of this measurement in terms of hazardous aircraft icing is discussed.

1. Introduction

The concept of drizzle growth by a combination of condensation and collision-coalescence has long been recognized in cloud environments where the temperature is warmer than 0°C (see, e.g., Langmuir 1948; Ludlum 1951). Pruppacher and Klett (1978) gives a historical overview of work in this area, while Beard and Ochs (1993) provides a more current review. This phenomenon has also been inferred in several studies for clouds in which the temperature of the cloud environment was colder than 0°C . The latter observations fall into two categories: observations of supercooled drizzle at the ground, combined with radiosonde measurements that indicated a source cloud layer that was entirely cooler than 0°C (Ohtake 1963; Bocchieri 1980; Huffman and Norman 1988); and in situ aircraft-based observations of supercooled drizzle-sized drops in convective and stratiform clouds (Byers 1952; Braham 1964; Isaac and Schemenauer 1979; Sand et al. 1984; Politovich 1989; Pobanz et al. 1994).

In each case, the growth of supercooled drizzle drops larger than $100\text{ }\mu\text{m}$ in diameter was inferred to have occurred through a condensation and collision-coalescence process. Strong moisture sources and vertical lift have been suggested to be necessary for the growth of such drops (Langmuir 1948; Ludlum 1951; Pruppacher and Klett 1978; Politovich 1989), while the simultaneous inefficiency of the ice phase has been explained by observations that the minimum cloud temperatures were usually warmer than -10°C and that there was a relative lack of active ice nuclei at such temperatures (Ohtake 1963; Braham 1964; Bocchieri 1980; Huffman and Norman 1988; Politovich 1989). Pobanz et al. (1994) have suggested that wind shear is often associated with the formation of large drops. However, few studies have provided in-depth documentation of the microphysics associated with the growth and evolution of supercooled drizzle drops. Rasmussen et al. (1995) have documented a recent example in shallow upslope clouds in Colorado.

On a research flight during the Second Canadian Atlantic Storms Program (Stewart 1991), an instrumented aircraft entered a region of drizzle at -7.5°C at an altitude of 3100 m. Because of an excessive buildup of ice on the aircraft, an ascent was performed to exit from the icing region. The vertical profile obtained extended completely through the cloud in which the drizzle formed and provided a characterization of the evo-

Corresponding author address: Dr. Stewart Cober, Cloud Physics Research Division, ARMP, Atmospheric Environment Service, 4905 Dufferin Street, Downsview, ON M3H 5T4, Canada.
E-mail: cobers@aestor.am.doe.ca

lution of the drizzle drops in an environment that was entirely colder than -7°C . The microphysics associated with the formation and growth of the drizzle drops are reported and discussed here. The measurements are discussed in terms of the associated hazard to aircraft and are compared to the standard icing curves used for aircraft certification.

2. Instrumentation

The research aircraft was a Convair-580 operated by the National Research Council of Canada. It was equipped by the Atmospheric Environment Service (AES) for cloud microphysics measurements as described in Cober et al. (1995). Instrumentation included the following: two Rosemount temperature probes and a reverse flow temperature probe, which generally agreed to within 1°C ; a Cambridge dewpoint hygrometer, which measured dewpoint to within $\pm 2^{\circ}\text{C}$; a Particle Measuring System (PMS) forward-scattering spectrometer probe (FSSP) 100, which measured concentrations ($\pm 20\%$) of droplet sizes between 1.5 and $49\ \mu\text{m}$ in diameter; a passive cavity aerosol spectrometer probe (PCASP), which measured aerosol spectra ($0.13\text{--}3\ \mu\text{m}$); two PMS King probes (King et al. 1978), which measured liquid water content (LWC) to $\pm 0.02\ \text{g m}^{-3}$ for LWC less than $0.2\ \text{g m}^{-3}$; a Rosemount 871FA221B icing detector; an icing cylinder from which ice buildup could be measured from video tape images to $\pm 1\ \text{mm}$; a Rosemount 858 gust probe; a PMS 2DC mono probe ($25\text{--}800\ \mu\text{m}$); a PMS 2DC gray ($25\text{--}1600\ \mu\text{m}$); and a PMS 2DP mono ($200\text{--}6400\ \mu\text{m}$). The three PMS 2D probes provided shapes and concentrations of hydrometeors within their respective size ranges. Horizontal winds were also measured with a Litton 91 IRS navigational system.

While the instruments collectively allow detailed characterizations of the microphysics of the cloud environment crossed by the aircraft, there are significant deficiencies in the instrumentation associated with the measurements of drops in the size range between 50 and $150\ \mu\text{m}$. The FSSP sized droplets only up to $49\ \mu\text{m}$, while depth of field errors associated with the channels from 25 to $150\ \mu\text{m}$ (lowest six channels) of the 2DC mono and 2DC gray probes cause significant uncertainty in the concentrations measured in these channels, particularly in the channels below $100\ \mu\text{m}$. In addition, the 2D probes may also incorrectly size drops (Joe and List 1987; Korolev et al. 1991), an effect that can be significant for drops smaller than $100\ \mu\text{m}$ in diameter. Consequently, the measurements of drops in the first four channels of the 2DC mono and 2DC gray were ignored in this analysis, so that there is a measurement gap between 50 and $125\ \mu\text{m}$. The 2DC drop spectra larger than $125\ \mu\text{m}$ were not corrected to account for oversizing, as demonstrated by Korolev et al. (1991). For similar reasons, measurements of concentrations based on 2DP data do not incorporate data

from the first two channels and, consequently, reflect only particles greater than $500\ \mu\text{m}$ in diameter.

Ice buildup on instruments can have a significant effect on their measurements. The majority of the instruments are heated to avoid this problem, and several probes were modified by AES to augment icing protection. The data from each instrument was carefully examined for indications of ice buildup. Icing in the drizzle region was not enough to significantly affect the FSSP, PCASP, or 2D probes, although the Rosemount 858 probe was affected, and its data was not used in the analysis.

3. Measurements and discussion

a. Synoptic situation

On 14 March 1992, an upper-level low pressure circulation centered over Labrador dominated the synoptic pattern near Newfoundland (see Fig. 1a). The winds at 70 kPa in the flight region were predominately from the south and southwest, which was consistent with the circulation around the upper-level low. A 99.2-kPa low pressure center (Fig. 1b) was associated with a wave that had evolved from the circulation of the upper-level feature. The aircraft flew north of the redeveloping low pressure region, although at the initial flight level of 68 kPa, the aircraft was well above the frontal surface. Winds at 68 kPa ($3100\ \text{m}$) were from the southwest (210°) at $13\ \text{m s}^{-1}$, while winds at 59.5 kPa ($4200\ \text{m}$) were from the south (170°) at $42\ \text{m s}^{-1}$, which represented a large vertical wind shear. In the location where the aircraft encountered the drizzle, the vertical velocity was between 4 and $7\ \text{cm s}^{-1}$ based on calculations from the Canadian Regional Finite Element Model (Benoit et al. 1989). This is consistent with the trough in Fig. 1b, which indicates a region of large-scale ascent. The aircraft location coincides well with the region of lifting above the frontal surface.

b. Microphysics measurements

During level flight heading east from St. John's (Fig. 1), the aircraft encountered drizzle drops at an altitude of $3150\ \text{m}$ (-7.5°C) at 1329 UTC 14 March 1992. An ascent was started at 1331:30 UTC, reaching $4230\ \text{m}$ (-11°C) at 1337 UTC. Cloud base was entered at 1330 UTC, just before starting the ascent, and cloud top was exited at 1340 UTC. Between 1337 and 1340 UTC, the aircraft flew level, below cloud top. The cloud-top height was observed from the aircraft to decrease from west to east. Consequently, while the cloud-top temperature measured from the aircraft at 1340 UTC was -11°C , the cloud-top temperature to the west, above the region where the drizzle was observed, was probably colder than -11°C by $1^{\circ}\text{--}2^{\circ}\text{C}$. The aircraft profile was roughly perpendicular to the winds, so that the measurements should be unbiased with respect to the cloud and drizzle drop trajectories. The horizontal ex-

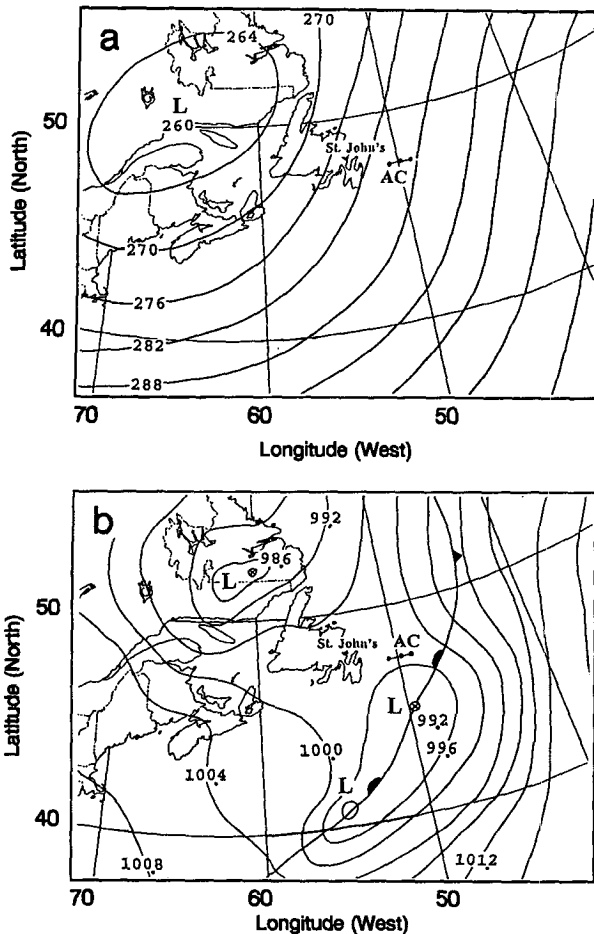


FIG. 1. Analysis of 1200 UTC 14 March 1992 for (a) 70-kPa geopotential height and (b) mean sea level surface pressure. Geopotential height contours are labeled in tens of meters, and mean sea level pressures are in kilopascals. The aircraft location between 1320 and 1340 UTC is marked AC.

tent of the drizzle region crossed by the aircraft between 1330 and 1337 UTC was approximately 40 km. To link microphysical measurements at different altitudes, the subsequent analysis assumes that the hori-

zontal cloud environment was relatively constant across the 40 km. The microphysics measurements and hydrometeor evolution discussed below support this assumption.

Time history graphs of LWC from the King probe and altitude are shown in Fig. 2. Images of hydrometeors from the 2DC mono and 2DP are shown in Figs. 3 and 4, respectively, for selected times in Fig. 2 (points A–K). Figures 3 and 4 include zero area images, shattered drops, and out of focus images, all of which are rejected when a quantitative analysis is performed on the 2D data. Prior to 1327 UTC the aircraft flew through a region of glaciated cloud, characterized by no LWC, 2DP ice crystal concentrations (>0.5 mm in diameter) of 0.2 L^{-1} , and PCASP aerosol concentrations ($>0.13 \mu\text{m}$) of $40\text{--}60 \text{ cm}^{-3}$. The ice crystal images were mainly 1–4-mm dendrites, and no drops were discernible in the 2DC or 2DP images. Between 1327 and 1329 UTC, the PCASP concentrations dropped to 5 cm^{-3} , while the crystal nature remained relatively unchanged (points A and B), although the 2DP concentration decreased to 0.08 L^{-1} . Between 1329 and 1330 UTC, the 2DC images showed an evolution to circular particles (points C and D), and by 1330 UTC, there were only a few small irregular images on the 2DP, while the 2DC was showing mainly drizzle drops with maximum diameters of $500 \mu\text{m}$. Hydrometeors of less than $500\text{-}\mu\text{m}$ diameter would shadow too few photo diodes to distinguish drops from crystals on the 2DP because of the $200\text{-}\mu\text{m}$ resolution of the probe. The large number of blank images in Figs. 4d–i is an indication of very small particles (less than roughly $200 \mu\text{m}$), which trip the electronics but pass out of the sample volume before they can be imaged. This, with the simultaneous lack of large numbers of larger images, is consistent with the existence of drizzle drops. It is evident that by 1330, the majority of the 2DC images were circular with diameters of less than 0.5 mm. The transition from crystals to drops was observed across a 10-km region. The aircraft continued with level flight until 1331:30 UTC (points E and F), when an ascent was started to exit from the drizzle region. A region with supercooled cloud droplets was

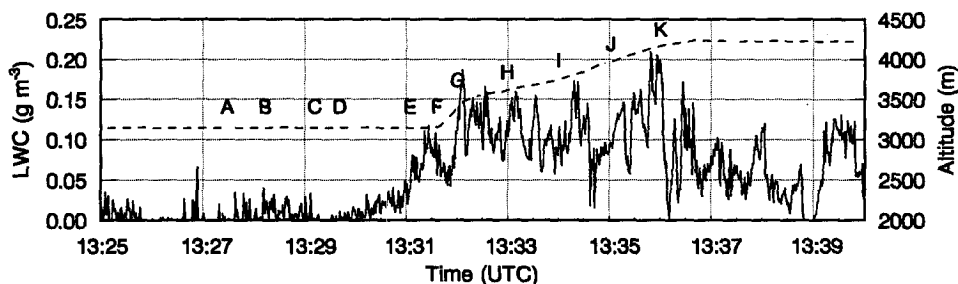


FIG. 2. Time history of King LWC (solid line) and altitude (dashed line) between 1325 and 1340 UTC. Points A–K correspond to the times of 2DC and 2DP images shown in Figs. 3 and 4, respectively.



FIG. 3. The 2DC mono images at selected times between 1327 and 1336 UTC. The vertical lines separating images represent a scale length of $800 \mu\text{m}$. Images without any recognizable particle are likely caused by the probe triggering on a droplet that is roughly one photo diode ($25 \mu\text{m}$) in diameter and consequently too small to resolve as an image. Some irregular images are caused by hydrometeors that are out of focus.

entered at 1330 UTC as indicated by an increase in the FSSP droplet concentrations and King probe LWC (Fig. 2). Figures 3f–j show a decrease in the 2DC drop sizes as the aircraft ascended through the cloud, and by 1336 (Fig. 3k) the drops were too small to resolve their shapes with the 2DC. In the upper regions of the cloud (points J and K), the 2DP measured concentrations of 0.08 L^{-1} for ice particles with diameters larger than 0.5 mm . No 2D images are shown after 1337 UTC because the images are similar to those in frames k of Figs. 3 and 4.

The temperature profile measured by the aircraft between 3150 and 4230 m around 1335 UTC is shown in Fig. 5, along with a more complete vertical profile taken at 1520 UTC, about 300 km north of the area where the drizzle was measured. No layer warmer than 0°C was observed in either profile, implying that the drizzle drops did not form through a melting process. Vertical profiles through the drizzle region of LWC, FSSP droplet concentration, FSSP droplet mean vol-

ume diameter, and wind speed and direction are shown in Fig. 6. Figure 6a shows that the aircraft was in liquid cloud throughout the ascent, with an LWC between 0.05 and 0.2 g m^{-3} . The FSSP droplet concentration varied between 10 and 20 cm^{-3} below 3800 m , and increased with altitude to 40 cm^{-3} at 4000 m . The mean volume diameter of cloud droplets was $22 \mu\text{m}$ and was relatively constant with altitude, although this is based on FSSP measurements that do not include contributions from drops larger than $49 \mu\text{m}$. An increase in the mean volume diameter to values greater than $25 \mu\text{m}$ at 3800 m is well correlated with a corresponding decrease in the droplet concentration. High mean volume diameters at 3800 and 4200 m may indicate that these areas are favorable source regions for the initiation of drizzle.

The PCASP aerosol spectra (0.13 – $3 \mu\text{m}$) are shown in Fig. 7. The average spectrum in glaciated cloud prior to the drizzle region (curve A) had a concentration of 38 cm^{-3} , with a mean volume diameter of $1.0 \mu\text{m}$. In

A. 2D-P mono TIME: 13:27:26:050



B. 2D-P mono TIME: 13:28:13:525



C. 2D-P mono TIME: 13:29:10:550



D. 2D-P mono TIME: 13:29:37:550



E. 2D-P mono TIME: 13:31:03:550



F. 2D-P mono TIME: 13:31:33:550



G. 2D-P mono TIME: 13:31:57:550



H. 2D-P mono TIME: 13:32:57:550



I. 2D-P mono TIME: 13:33:58:050



J. 2D-P mono TIME: 13:35:04:450



K. 2D-P mono TIME: 13:35:58:850



FIG. 4. The 2DP images at the same selected times as in Fig. 3. The vertical spacing lines represent a scale length of 6.4 mm.

the liquid cloud region (curve B), the concentration was 11 cm^{-3} with a mean volume diameter of $1.9 \mu\text{m}$. The reduction in the aerosol concentration is consistent with the aerosol particles acting as cloud condensation nuclei (CCN), although some may have been scavenged by the drizzle drops. The change in the PCASP concentration from 38 to 11 cm^{-3} is roughly consistent with the average cloud drop concentration of 21 cm^{-3} and supports the contention that the aerosols larger than $0.13 \mu\text{m}$ were serving as CCN. Aerosol concentrations of this magnitude in this size range are extremely low and are indicative of clean background concentrations (Leitch and Isaac 1991). A water sample was collected with a heated cloud water collector immediately after leaving the drizzle region. It is believed that the sample resulted from drizzle drops that froze upon impaction with the collector and subsequently melted into the collection bottle. The sample was analyzed for major inorganic ions. Sulphate, chloride, sodium, and potassium were below detection level [detection levels were, respectively, 3.4, 0.8, 1.0, and 1.5 microequivalents per liter ($\mu\text{E L}^{-1}$)], while nitrate and ammonium were present at about twice detection levels ($2 \mu\text{E}$

L^{-1}). These concentrations are very low in comparison to similar measurements in other cloud studies (Leitch et al. 1992) and support the idea that the air mass was quite clean.

The FSSP spectra are shown in Fig. 8 for 6-min averages taken before the aircraft entered the drizzle region (curve A) and for the ascent profile (curve B). Curve A likely shows the FSSP response to ice crystals (Gardiner and Hallett 1985) as there are nearly equal particle concentrations for $14 \mu\text{m}$ and larger. The in-cloud droplet distribution (curve B) had an average concentration of 21 cm^{-3} , mean volume diameter of $22 \mu\text{m}$, and median volume diameter of $29 \mu\text{m}$. The concentration of droplets larger than $40 \mu\text{m}$ averaged 300 L^{-1} throughout the cloud.

The evolution of the FSSP and 2DC spectra are given in Fig. 9 for 90–180-s averages, which correspond to specific altitude intervals. The FSSP and 2DC spectra are interpolated between the last channel of the FSSP and the fifth channel of the 2DC. The 2DC concentrations in the 25-, 50-, 75-, and $100\text{-}\mu\text{m}$ channels are not shown because of the large errors associated with both sizing and concentrations in these channels.

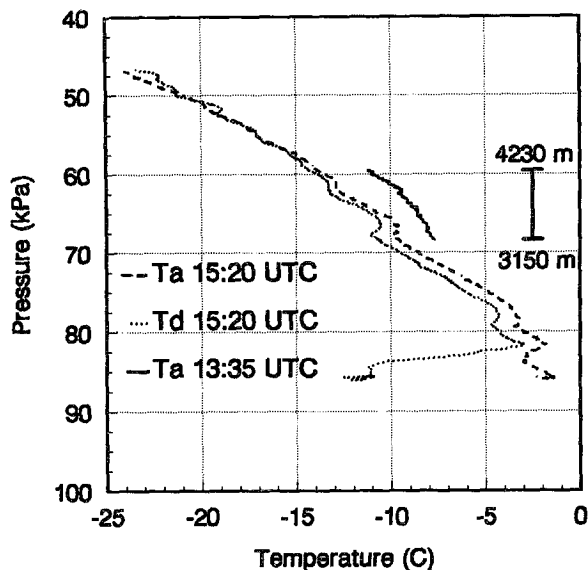


FIG. 5. Vertical temperature profile of the ascent through the drizzle region at 1335 UTC (solid curve). The altitude spanned 3150–4230 m, which is labeled for comparison to Fig. 6. Vertical profiles of temperature (dashed curve) and dewpoint (dotted curve) measured at 1520 UTC are shown for comparison. The latter measurements were made with the aircraft approximately 2 h after the profile through the drizzle region and approximately 300 km further north.

The analysis of 2DC data was performed with a center-in technique similar to that described by Heymsfield and Parrish (1978), with acceptance of particles with box-area ratios greater than 0.65 and box-axis ratios between 1.0 and 1.5. The rejection criteria discussed above are effective in screening out noncircular im-

ages, out of focus particles, and zero area images, thereby leaving presumably only well-imaged drizzle drops for numerical analysis. A careful inspection of all 2D records during the period spanning frames (e)–(k) (Figs. 3 and 4) showed two distinct populations, small circular drizzle drops and larger noncircular ice crystals. The existence of drizzle drops below cloud base was verified by the icing signature on the icing rod and the Rosemount icing detector, and it is reasonable to assume that these are from the same population as those observed in-cloud. It is unlikely that significant numbers of the small in-cloud circular images are ice crystals, since it is improbable that small crystals with near-circular faces would coexist with drizzle drops to a maximum diameter of 500 μm and then reappear at much larger diameters with a dendritic structure. In this water-saturated environment, ice crystals would grow quickly to millimeter sizes. Thus using the restrictive acceptance criteria summarized above should eliminate all of the larger noncircular ice crystals and leave only the small circular images that are interpreted to be drizzle drops.

Curve A (Fig. 9) represents drizzle measurements taken at cloud base (altitude 3150 m), while curve D represents measurements near cloud top (4160–4220 m). Curves B and C represent averages through the lower (3150–3615 m) and upper (3615–4160 m) halves of the cloud, respectively. The FSSP concentrations were highest in the upper half of the cloud, where the 2DC measurements showed a relative absence of drizzle drops. Conversely, the drizzle spectra clearly evolve to larger sizes from cloud top to cloud base. These observations are consistent with growth by collision-coalescence. The cloud-top region was the

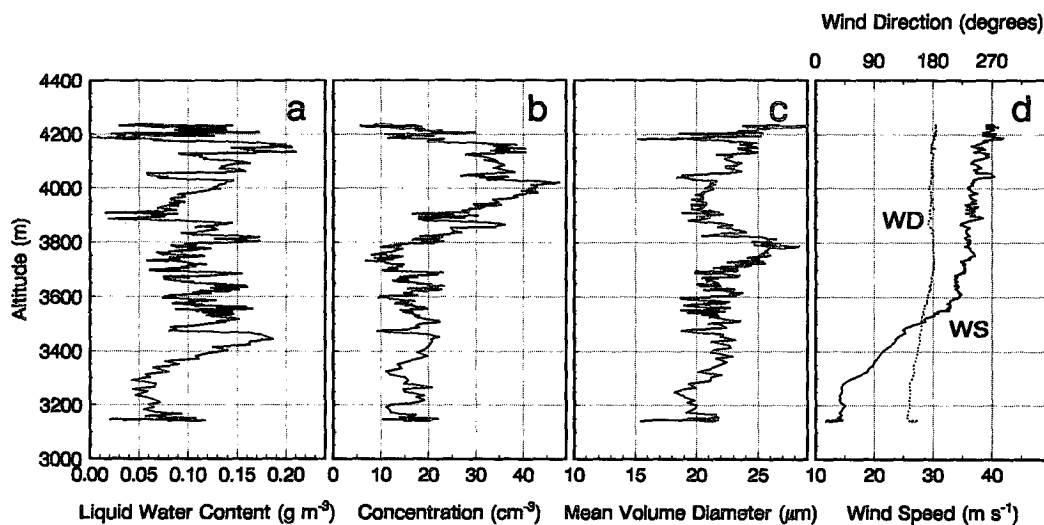


FIG. 6. Vertical profiles for the ascent between 1331:30 and 1337:00 UTC: (a) King probe LWC, (b) FSSP droplet concentration, (c) FSSP mean volume diameter, and (d) wind speed (WS) and direction (WD). The entire ascent was in cloud. The temperature profile for this region is shown in Fig. 5.

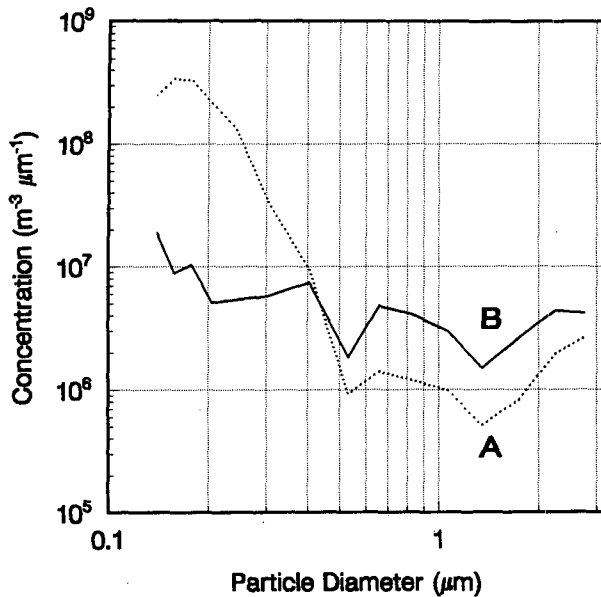


FIG. 7. Six-minute-averaged PCASP spectra for (a) the region of glaciated cloud immediately prior to the drizzle region (1322–1328 UTC) and (b) the vertical profile through the drizzle and cloud region (1331–1337 UTC).

source region for some of the drizzle drops, which grew by collision-coalescence once their terminal velocity exceeded the upward vertical velocity. The temperature in this region was -11°C . Although ice particles were observed with the 2DP throughout the cloud region (concentrations of 0.08 L^{-1} for particles larger than 0.5 mm), they were ineffective in glaciating the cloud and drizzle region.

Photographs of the icing cylinder indicated that $6.0 \pm 1.5\text{ mm}$ of ice built up between 1330 and 1337 UTC. This implies an average LWC of $0.12 \pm 0.03\text{ g m}^{-3}$, assuming an ice density of 0.8 g cm^{-3} . The King probe (short wire version) average LWC for the same period was 0.09 ± 0.02 . The difference may be associated with the large errors in measuring the ice thickness and uncertainty in the ice density. In addition, the King probes are known to underestimate the LWC incorporated in drops greater than $50\text{ }\mu\text{m}$ (Biter et al. 1987). Therefore, considering the uncertainties noted above, the measurements of the icing rod and the King probe are consistent.

Because of the enhanced aircraft icing hazard associated with supercooled drizzle drops, as compared to that from supercooled cloud droplets (see section 4), it is useful to determine the fraction of the LWC incorporated in drops larger than $50\text{ }\mu\text{m}$ in diameter. Using the 2DC and interpolated LWC as described above, the total LWCs for curves A–D in Fig. 9 were 0.06 ± 0.02 , 0.14 ± 0.03 , 0.12 ± 0.02 , and $0.08 \pm 0.02\text{ g m}^{-3}$, respectively, of which 62%, 53%, 17%, and 6% of the LWC was associated with drops larger than $50\text{ }\mu\text{m}$.

Figure 10 gives the fraction of mass incorporated in drops smaller than a specified size and demonstrates the evolution of the LWC from cloud droplets to drizzle drops as the drizzle moved lower in the cloud. At cloud base (curve A), roughly 56% of the mass was incorporated in drops larger than $100\text{ }\mu\text{m}$. Conversely, at cloud top (curve D), over 95% of the mass was in droplets smaller than $50\text{ }\mu\text{m}$. The uncertainties in concentrations and sizing for the 2DC mono, and in the interpolation of the droplet spectrum between 50 and $125\text{ }\mu\text{m}$, cause the LWC estimates for drops greater than $50\text{ }\mu\text{m}$ to be accurate within a factor of 2. Regardless, these errors do not affect the trends observed in the evolution of the drop spectra from cloud top to cloud base as shown in Fig. 10.

c. Simple growth calculations

Johnson (1980) has modeled the evolution of droplet spectra from an initial aerosol spectra. This model was applied to the conditions of the case study reported here. It predicted that a droplet distribution with a concentration of 24 cm^{-3} , mean volume diameter of $25\text{ }\mu\text{m}$, and liquid water content of 0.2 g m^{-3} could be obtained within 200 m from cloud base, assuming a cloud-base temperature of -8°C , adiabatic lifting of 0.1 m s^{-1} , and a maritime aerosol distribution with a concentration of aerosols greater than $0.13\text{ }\mu\text{m}$ equal to 11 cm^{-3} . These values are quite similar to those measured in this case. Unfortunately, the vertical velocity in the drizzle region could not be measured from the aircraft, although the vertical velocity of the air mass

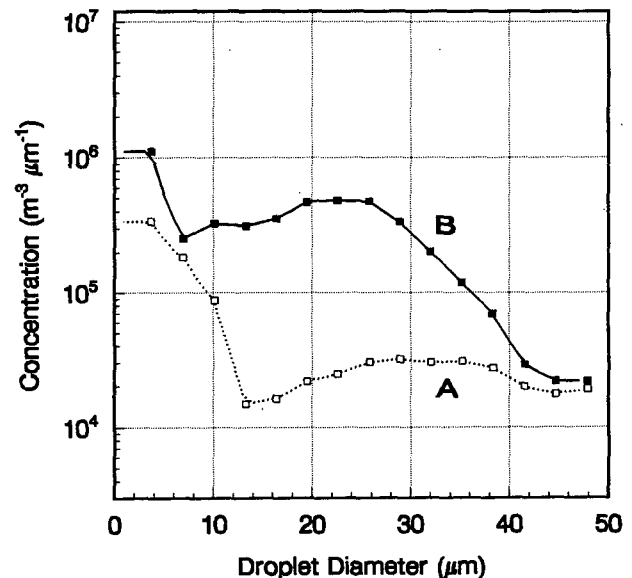


FIG. 8. Six-minute-averaged FSSP spectra corresponding to the same intervals as in Fig. 7. The first channel of the FSSP is biased because of noise problems.

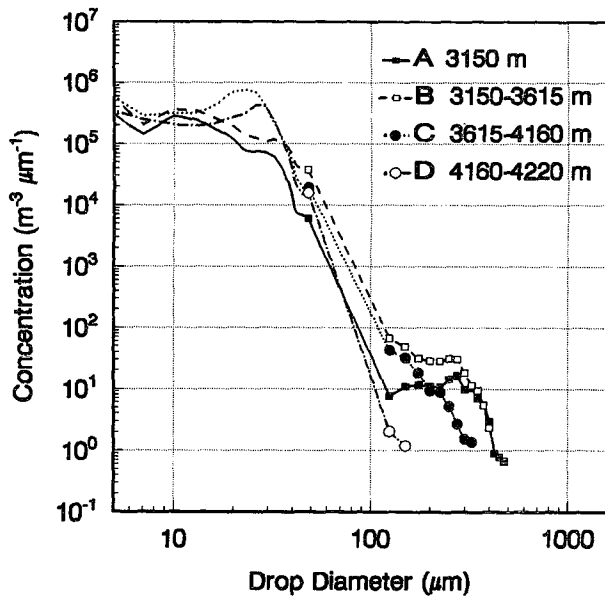


FIG. 9. FSSP and 2DC spectra averaged over 90–180-s periods, which correspond to specific altitude intervals: (A) level flight at 3150 m between 1330:00 and 1331:30 UTC, (B) profile from 3150 to 3615 m between 1331:30 and 1333:00 UTC, (C) profile from 3615 to 4160 m between 1333:00 and 1336:00 UTC, and (D) level flight between 4160 and 4220 m between 1336:00 and 1337:30 UTC. Measurements from the last FSSP channel and from each 2DC channel are also shown, although data from the first four 2DC channels have been ignored. The linear interpolation between the FSSP and fifth channel of the 2DC is included in the curves, although it does not represent actual data.

was estimated to be between 5 and 7 cm s^{-1} (section 3a). It is likely that local updrafts had larger vertical velocities, although the stratiform nature and wide horizontal extent of the clouds implied low vertical velocities overall. The temperature profile in the drizzle region followed a saturated adiabatic lapse rate, although the liquid water content was not adiabatic throughout the cloud. Drizzle drops growing from collision-coalescence would tend to reduce and redistribute the liquid water content significantly. In the model simulation, the droplet spectrum took 30 min to reach a height of 200 m above cloud base, at which point the supersaturation S predicted by the model was relatively constant at 0.15%. Further growth to diameters of 40 μm at $S = 0.15\%$ took an additional 30 min, assuming only condensational growth.

Using the collection efficiencies of Beard and Ochs (1984), a 100- μm drop was modeled falling from cloud top (4200 m) to cloud base (3100 m), through a cloud with a median volume diameter of 29 μm and a LWC of 0.1 g m^{-3} . The drop took 45 min to fall, during which time it grew to 170 μm in diameter. Such an increase is consistent with the observed change in the 2DC mean volume diameter (drops greater than 100 μm only), which varied from 112 μm at cloud top to

260 μm at cloud base. The calculated change is smaller, but does not take into account the observed increase in concentration and sizes of drizzle drops lower in the cloud, updraft velocities larger than 0.1 m s^{-1} , or stochastic coalescence processes. Oversizing by the 2DC probe also accounts for some of the difference.

The evolution of the cloud droplet spectrum to droplets larger than 40 μm has been discussed in detail in Pruppacher and Klett (1978). They indicated that the production of droplets of 40–50 μm in diameter in concentrations of several per liter was an important step in the stochastic coalescence process for the evolution of larger drops, which could then grow by geometric sweep out. The average FSSP droplet concentration between 1331 and 1337 UTC (Fig. 8, curve B) for droplets between 40 and 49 μm was 300 L^{-1} , which is two orders of magnitude larger than the necessary concentrations given by Pruppacher and Klett (1978). No attempts have been made to estimate the processes whereby droplets between 40 and 100 μm are formed. As outlined by Beard and Ochs (1993), this remains a poorly understood phenomenon and is not addressed in this work. The lack of measurements in the 50–125- μm range prevents investigation of the link between the cloud droplets and the evolution of the drizzle drops, and represents an unavoidable limitation of this work. Avoiding estimating the time required for the stochastic coalescence of drops between 40 and 100 μm is equivalent to assuming that this process took place simultaneously with the other processes.

Pobanz et al. (1994) have suggested that the development of large drops is linked to regions of wind

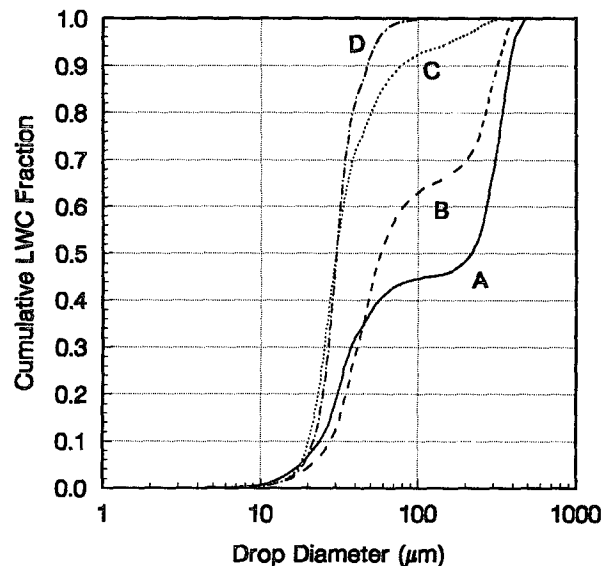


FIG. 10. Cumulative mass curves for FSSP and 2DC spectra for the same altitude and time intervals shown in Fig. 9. The LWC values for curves A, B, C, and D are 0.06, 0.14, 0.12, and 0.08 g m^{-3} , respectively.

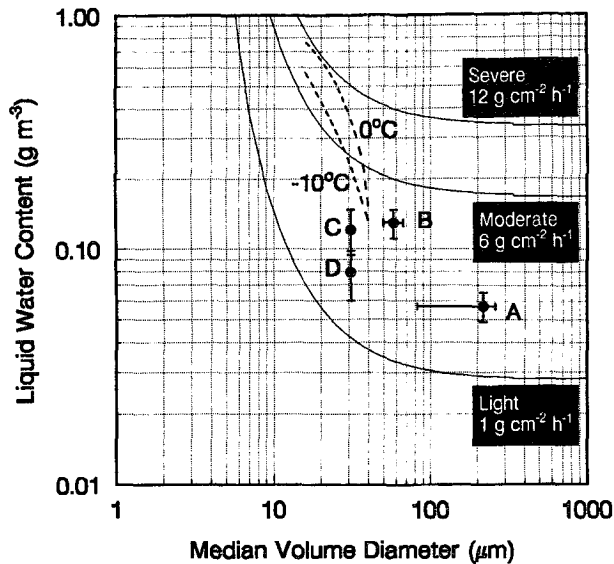


FIG. 11. Median volume diameter versus LWC for the same FSSP/2DC spectra plotted in Fig. 10. The median volume diameter for each spectrum corresponds to the cumulative LWC fraction of 0.5 in Fig. 10. Solid curves represent the icing curves of Newton (1978) for light, moderate, and severe icing. Dashed curves represent the maximum continuous icing curves from FAR 25-C for 0° and -10°C. Points A–D correspond to the same altitude/time intervals as in Figs. 9 and 10. The Newton curves represent the maximum potential accumulation of ice ($\text{g cm}^{-2} \text{h}^{-1}$) on a 7.6-cm cylinder, at an airspeed of 100 m s^{-1} , at -10°C, and at 70.0 kPa.

shear, with the shear causing inhomogeneous mixing and turbulence, leading to the formation of large drops. In this case, there was a strong wind shear of 0.05 s^{-1} in the lowest 300 m of the cloud, with a corresponding Richardson number of 0.10. In the upper half of the cloud there was a 200-m layer with a Richardson number of 0.35 and shear of 0.02 s^{-1} . Both regions are consistent with the discussion of Pobanz et al. (1994), who inferred that regions with shear greater than 0.02 s^{-1} and Richardson numbers smaller than 1 were highly correlated with regions in which large drops formed. Conversely, there was no significant shear region near cloud top as hypothesized by Pobanz et al. (1994), and 100- μm drops were also measured within 100 m of cloud top where the shear was 0.01 s^{-1} and the Richardson number was 3. Hence, the mechanism of Pobanz et al. (1994) was not necessarily active in this case.

While it is not the intent of this work to fully model the growth of the measured drizzle spectrum, these calculations have been performed to show that the measurements support the concept that the drizzle grew by a condensation and collision-coalescence process, and to provide an estimate of the timescale for the formation of the drizzle drops. Using the simple time estimates given above, and neglecting the stochastic coalescence processes for drops between 40 and 100 μm ,

the minimum times necessary for the evolution of the cloud droplet spectra by condensation and drizzle spectra by collision coalescence was roughly 1–2 h. This is not unreasonable given the low liquid water content of the cloud. Low aerosol concentrations produced a cloud drop distribution with a low concentration and large median volume diameter, with a significant tail of drops larger than 40 μm , which initiated the collision-coalescence process.

These observations imply that the cloud remained supercooled for a period of 1–2 h without being significantly glaciated. Ice particle concentrations of 0.08 L^{-1} (greater than 0.5 mm in diameter) were measured throughout the cloud and drizzle region. At -12°C, the expected mean concentration of active ice nuclei is roughly 0.01 L^{-1} , within one order of magnitude (Pruppacher and Klett 1978), which is consistent with the measured concentration of ice particles measured with the 2DP. Assuming saturation with respect to water, the supersaturation with respect to ice is 12% at -12°C. Dendritic plates of 2-mm diameter would grow in approximately 1 h under these conditions, which is consistent with the images seen on the 2DP (Figs. 4g–k) throughout the cloud. The lack of small crystals implies the absence of an effective ice multiplication mechanism in the cloud region where the drizzle was measured. The temperature of the drizzle region (-7.5° to -11°C) was too cold for the ice multiplication mechanism described by Hallett and Mossop (1974) and Mossop (1976).

4. Application

Supercooled drizzle has long been recognized as presenting a significant hazard to aircraft (Lewis 1951). Icing causes a decrease in lift and increase in drag, and a rapid accumulation of ice could obscure visibility from the cockpit. These problems are most dangerous during takeoff or landing, when visibility is critical, and when the aircraft is closest to its stall speed. Drizzle-sized drops have a significantly greater collision efficiency with aircraft surfaces than cloud droplets, and therefore cause a faster buildup of ice for equivalent liquid water contents. In-flight observations of aircraft icing caused by supercooled drizzle have been reported by Sand et al. (1984) and Politovich (1989). They noted that the drizzle drops can flow back over and under the wings and behind deicing boots and suggested that such icing caused significantly more degradation of aircraft performance than icing caused by cloud droplets, for equivalent liquid water contents.

Figure 11 shows the liquid water contents versus the median volume diameters for the four curves in Fig. 9. The 2DC and FSSP data were interpolated together to derive the median volume diameters. The icing safety thresholds of the U.S. Federal Aviation Administration regulation 25 appendix C (FAR 25-C) and Newton (1978) are overlaid for comparison. For both sets of

curves, the larger the LWC and median volume diameter, the heavier the icing intensity. The FAR 25-C curves physically represent 0.1% exceedance probabilities for flight in continuous icing over 32.6 km and are used as an estimate of the maximum possible icing. While the FAR 25-C curves do not extend beyond 40 μm , it is evident that the flight lower in the cloud (points A and B) significantly exceeded the FAR 25-C thresholds. Conversely, the icing was not even classified as moderate under the Newton scheme, which contradicts the assessment of the FAR 25-C curves. During 119 h of in-flight measurements in winter storms over the North Atlantic Ocean (Cober et al. 1995), there were only three occasions in which icing was subjectively assessed as severe and the flight path was modified to exit from the icing region. Two of these (one of which is the case described here) occurred in the presence of supercooled drizzle, which formed through a collision-coalescence process. In both cases, the visual assessment by the pilots was that the icing was an unusual and potentially unsafe event, and they took immediate action to direct the aircraft out of the icing region. Their observations and reactions qualitatively support the FAR 25-C icing curves.

Freezing drizzle is frequently observed on the Canadian east coast in the winter (McKay and Thompson 1969). A climatology of freezing precipitation (Strapp et al. 1996) found that St. John's, Newfoundland, has the highest frequency of freezing precipitation in Canada, receiving 103 h of freezing drizzle and 51 h of freezing rain per year. The maximum frequency occurred in March when freezing precipitation was measured on the ground an average of 40 h per month, or 5.5% of the total hours. Strapp et al. (1996) have used radiosonde data and surface observations to show that approximately two-thirds of the freezing drizzle observed at the surface in St. John's forms through a collision-coalescence process, while one-third forms through ice particles melting and subsequently supercooling. Observations of freezing drizzle at St. John's, formed without a melting layer, were highly correlated with onshore winds. Strapp et al. (1996) inferred that such clean maritime air masses were suitable for the formation of supercooled drizzle through a condensation and collision-coalescence process. Ohtake (1963) also noted that freezing drizzle events with no warm layer aloft were correlated with winds from the ocean. The example discussed in this study, although not from low-level clouds during onshore winds, shared many of the same characteristics favorable for drizzle formation by condensation and coalescence.

The FAR 25-C curves represent the maximum icing conditions expected during 99.9% of icing encounters. The curves are based on in-flight icing cylinder measurements taken during the 1940s and do not distinguish median volume diameters greater than 40 μm . Certainly, cloud regions with supercooled drizzle can have median volume diameters larger than 40 μm , as

illustrated by the case described here. The high frequency of freezing drizzle on the east coast suggests that aircraft will be routinely taking off and landing in freezing drizzle conditions. These points suggest that the hazard to aircraft from supercooled drizzle is not adequately addressed in the safety thresholds of FAR 25-C. The hazard to aircraft is compounded by the inability of current forecast models to forecast supercooled drizzle in the absence of an associated melting layer.

5. Conclusions

Drizzle drops to 500 μm in diameter formed through a condensation and collision-coalescence process at temperatures between -11° and -8°C . The air mass was characterized by low aerosol concentrations (0.13–3 μm) of 40 cm^{-3} , while the cloud growth environment was characterized by an average droplet concentration of 21 cm^{-3} , interstitial aerosol concentrations of less than 15 cm^{-3} , and an average droplet median volume diameter of 29 μm . These observations are consistent with a clean air mass, with small numbers of droplets competing for available moisture. Consequently, the concentrations of cloud droplets with diameters larger than 40 μm exceeded 300 L^{-1} , which was sufficient for the initiation of growth by collision-coalescence. The evolution of the droplet spectra in the sizes smaller than 50 μm and greater than 125 μm was traced vertically through the cloud, and 500- μm drops were measured approximately 1000 m below the source region at cloud top. The ice particle concentration (greater than 0.5 mm in diameter) was 0.08 L^{-1} throughout the drizzle formation region. Simple growth models were used to estimate that the ice crystals and drizzle drops measured at cloud base had been growing for at least 1–2 h, and that no efficient ice multiplication mechanism was operating. Comparisons of the data with the aircraft icing curves of FAR 25-C have demonstrated a limitation with the accepted safety curves, which needs to be addressed. This study presents a well-documented example of drizzle-sized supercooled drops, which formed through a condensation–collision-coalescence process. Measurements of the hydrometeor spectra between 50 and 125 μm were not made, and represent a limitation of this work. Application of the microphysics data toward a better understanding of the stochastic coalescence process for drops in the 40–100- μm range is a subject for further research.

Acknowledgments. This work was funded by the Canadian National Search and Rescue Secretariat. Funding was also provided by Boeing Commercial Airplane Group, the Institute for Aerospace Research of the National Research Council of Canada, and the Atmospheric Environment Service (AES). The technicians and programmers of AES are acknowledged for their

support in keeping the instruments operational and calibrated, and for assistance provided in analyzing the 2D data. The NRC pilots are acknowledged for their safe and efficient operations of the Convair-580 aircraft. Thanks to Mike Patnoe for sharing the duties of flight director on this flight. Thanks also to Andre Tremblay for providing the vertical velocity data from the Regional Finite Element Model, and to Cathy Banic for providing the cloud water chemistry analysis.

REFERENCES

- Beard, K. V., and H. T. Ochs, 1984: Collection and coalescence efficiencies for accretion. *J. Geophys. Res.*, **89**(D), 7165–7169.
- , and —, 1993: Warm-rain initiation: An overview of microphysical mechanisms. *J. Appl. Meteor.*, **32**, 608–625.
- Benoit, R., J. Cote, and J. Mailhot, 1989: Inclusion of a TKE boundary layer parameterization in the Canadian regional finite-element model. *Mon. Wea. Rev.*, **117**, 1726–1750.
- Biter, C. J., J. E. Dye, D. Huffman, and W. D. King, 1987: The drop-size response of the CSIRO liquid water probe. *J. Atmos. Oceanic Technol.*, **4**, 359–367.
- Bocchieri, J. R., 1980: The objective use of upper air soundings to specify precipitation type. *Mon. Wea. Rev.*, **108**, 596–603.
- Braham, R. R., 1964: What is the role of ice in summer rain showers? *J. Atmos. Sci.*, **21**, 640–645.
- Byers, H. R., 1952: An example of flight through a thunderstorm updraft. *Bull. Amer. Meteor. Soc.*, **33**, 211–212.
- Cober, S. G., G. A. Isaac, and J. W. Strapp, 1995: Aircraft icing measurements in East Coast winter storms. *J. Appl. Meteor.*, **34**, 88–100.
- Gardiner, B. A., and J. Hallett, 1985: Degradation of in-cloud forward scattering spectrometer probe measurements in the presence of ice particles. *J. Atmos. Oceanic Technol.*, **2**, 171–180.
- Hallett, J., and S. C. Mossop, 1974: Production of secondary ice particles during the riming process. *Nature*, **249**, 26–28.
- Heymsfield, A. J., and J. L. Parrish, 1978: A computational technique for increasing the effective sampling volume of the PMS two-dimensional particle size spectrometer. *J. Appl. Meteor.*, **17**, 1566–1572.
- Huffman, G. J., and G. A. Norman, 1988: The supercooled warm rain process and the specification of freezing precipitation. *Mon. Wea. Rev.*, **116**, 2172–2182.
- Isaac, G. A., and R. S. Schemenauer, 1979: Large particles in supercooled regions of northern Canadian cumulus clouds. *J. Appl. Meteor.*, **18**, 1056–1065.
- Joe, P., and R. List, 1987: Testing and performance of two-dimensional optical array spectrometers with greyscale. *J. Atmos. Oceanic Technol.*, **4**, 139–150.
- Johnson, D. B., 1980: The influence of cloud-base temperature and pressure on droplet concentration. *J. Atmos. Sci.*, **37**, 2079–2085.
- King, W. D., D. A. Parkin, and R. J. Handsworth, 1978: A hot wire liquid water device having fully calculable response characteristics. *J. Appl. Meteor.*, **17**, 1809–1813.
- Korolev, A. V., S. V. Kuznetsov, Y. E. Makarov, and V. S. Novikov, 1991: Evaluation of measurements of particle size and sample area from optical array probes. *J. Atmos. Oceanic Technol.*, **8**, 514–522.
- Langmuir, I., 1948: The production of rain by a chain reaction in cumulus clouds at temperatures above freezing. *J. Meteor.*, **5**, 175–192.
- Leitch, W. R., and G. A. Isaac, 1991: Tropospheric aerosol size distributions from 1982 to 1988 over eastern North America. *Atmos. Environ.*, **25**, 601–619.
- , —, J. W. Strapp, C. M. Banic, and H. A. Wiebe, 1992: The relationship between cloud droplet number concentrations and anthropogenic pollution: Observations and climatic implications. *J. Geophys. Res.*, **97**(D), 2463–2474.
- Lewis, W., 1951: Meteorological aspects of aircraft icing. *Compendium of Meteorology*, T. F. Malone, Ed., Amer. Meteor. Soc., 1197–1203.
- Ludlum, F. H., 1951: The production of showers by the coalescence of cloud droplets. *Quart. J. Roy. Meteor. Soc.*, **77**, 402–417.
- McKay, G. A., and H. A. Thompson, 1969: Estimating the hazard of ice accretion in Canada from climatological data. *J. Appl. Meteor.*, **8**, 927–935.
- Mossop, S. C., 1976: Production of secondary ice particles during the growth of graupel by riming. *Quart. J. Roy. Meteor. Soc.*, **102**, 45–57.
- Newton, D. W., 1978: An integrated approach to the problem of aircraft icing. *J. Aircraft*, **15**, 374–380.
- Ohtake, T., 1963: Hemispheric investigation of warm rain by radiosonde data. *J. Appl. Meteor.*, **2**, 594–607.
- Pobanz, B. M., J. D. Marwitz, and M. K. Politovich, 1994: Conditions associated with large-drop regions. *J. Appl. Meteor.*, **33**, 1366–1372.
- Politovich, M. K., 1989: Aircraft icing caused by large supercooled droplets. *J. Appl. Meteor.*, **28**, 856–868.
- Pruppacher, H. R., and J. D. Klett, 1978: *Microphysics of Clouds and Precipitation*. Reidel, 714 pp.
- Rasmussen, R. M., B. C. Bernstein, M. Murakami, G. Stossmeister, and J. Reisner, 1995: The 1990 Valentine's Day arctic outbreak. Part I: Mesoscale and microscale structure and evolution of a Colorado Front Range shallow upslope cloud. *J. Appl. Meteor.*, **34**, 1481–1511.
- Sand, W. R., W. A. Cooper, M. K. Politovich, and D. L. Veal, 1984: Icing conditions encountered by a research aircraft. *J. Climate Appl. Meteor.*, **23**, 1427–1440.
- Stewart, R. E., 1991: Canadian Atlantic Storms Program: Progress and plans of the meteorological component. *Bull. Amer. Meteor. Soc.*, **72**, 364–371.
- Strapp, J. W., R. A. Stuart, and G. A. Isaac, 1996: A Canadian climatology of freezing precipitation, and a detailed study using data from St. John's Newfoundland. *Proc. FAA International Conf. on Aircraft Inflight Icing*, Springfield, VA, Federal Aviation Administration, in press.